

## Permutationally Invariant Quantum Tomography

G. Tóth,<sup>1,2,3</sup> W. Wieczorek,<sup>4,5,\*</sup> D. Gross,<sup>6</sup> R. Krischek,<sup>4,5</sup> C. Schwemmer,<sup>4,5</sup> and H. Weinfurter<sup>4,5</sup>

<sup>1</sup>*Department of Theoretical Physics, The University of the Basque Country, P.O. Box 644, E-48080 Bilbao, Spain*

<sup>2</sup>*IKERBASQUE, Basque Foundation for Science, E-48011 Bilbao, Spain*

<sup>3</sup>*Research Institute for Solid State Physics and Optics, Hungarian Academy of Sciences, P.O. Box 49, H-1525 Budapest, Hungary*

<sup>4</sup>*Max-Planck-Institut für Quantenoptik, Hans-Kopfermann-Strasse 1, D-85748 Garching, Germany*

<sup>5</sup>*Fakultät für Physik, Ludwig-Maximilians-Universität, D-80797 München, Germany*

<sup>6</sup>*Institute for Theoretical Physics, Leibniz University Hannover, D-30167 Hannover, Germany*

(Received 4 June 2010; revised manuscript received 30 August 2010; published 16 December 2010)

We present a scalable method for the tomography of large multiqubit quantum registers. It acquires information about the permutationally invariant part of the density operator, which is a good approximation to the true state in many relevant cases. Our method gives the best measurement strategy to minimize the experimental effort as well as the uncertainties of the reconstructed density matrix. We apply our method to the experimental tomography of a photonic four-qubit symmetric Dicke state.

DOI: 10.1103/PhysRevLett.105.250403

PACS numbers: 03.65.Wj, 03.65.Ud, 42.50.Dv

Because of the rapid development of quantum experiments, it is now possible to create highly entangled multiqubit states using photons [1–5], trapped ions [6], and cold atoms [7]. So far, the largest implementations that allow for an individual readout of the particles involve on the order of 10 qubits. This number will soon be overcome, for example, by using several degrees of freedom within each particle to store quantum information [8]. Thus, a new regime will be reached in which a complete state tomography is impossible even from the point of view of the storage space needed on a classical computer. At this point the question arises: Can we still extract useful information about the quantum state created?

In this Letter we propose permutationally invariant (PI) tomography in multiqubit quantum experiments [9]. Concretely, instead of the density matrix  $\varrho$ , we propose to determine the PI part of the density matrix defined as

$$\varrho_{\text{PI}} = \frac{1}{N!} \sum_k \Pi_k \varrho \Pi_k, \quad (1)$$

where  $\Pi_k$  are all the permutations of the qubits. Reconstructing  $\varrho_{\text{PI}}$  has been considered theoretically for spin systems (see, e.g., Ref. [10]). Recently it has been pointed out that photons in a single mode optical fiber will always be in a PI state and that there is only a small set of measurements needed for their characterization [11,12].

Here, we develop a provably optimal scheme, which is feasible for large multiqubit systems: For our method, the measurement effort increases only quadratically with the size of the system. Our approach is further motivated by the fact that almost all multipartite experiments are done with PI quantum states [2–4,6]. Thus, the density matrix obtained from PI tomography is expected to be close to the one of the experimentally achieved state. The expectation values of symmetric operators, such as some entanglement witnesses, and fidelities with respect to symmetric states are the same

for both density matrices and are thus obtained exactly from PI tomography [2–4]. Finally, if  $\varrho_{\text{PI}}$  is entangled, so is the state  $\varrho$  of the system, which makes PI tomography a useful and efficient tool for entanglement detection.

Below, we summarize the four main contributions of this Letter. We restrict our attention to the case of  $N$  qubits—higher-dimensional systems can be treated similarly.

(1) In most experiments, the qubits can be individually addressed whereas nonlocal quantities cannot be measured directly. The experimental effort is then characterized by the number of local measurement settings needed, where “setting” refers to the choice of one observable per qubit, and repeated von Neumann measurements in the observables’ eigenbases [13]. Here, we compute the minimal number of measurement settings required to recover  $\varrho_{\text{PI}}$ .

(2) The requirement that the number of settings be minimal does not uniquely specify the tomographic protocol. On the one hand, there are infinitely many possible choices for the local settings that are both minimal and give sufficient information to find  $\varrho_{\text{PI}}$ . On the other hand, for each given setting, there are many ways of estimating the unknown density operator from the collected data. We present a systematic method to find the optimal scheme through statistical error analysis.

(3) Next, we turn to the important problem of gauging the information loss incurred due to restricting attention to the PI part of the density matrix. We describe an easy test measurement that can be used to judge the applicability of PI tomography before it is implemented.

(4) Finally, we demonstrate that these techniques are viable in practice by applying them to a photonic experiment observing a four-qubit symmetric Dicke state.

*Minimizing the number of settings.*—We will now present our first main result.

**Observation 1.** For a system of  $N$  qubits, permutationally invariant tomography can be performed with

$$\mathcal{D}_N = \binom{N+2}{N} = \frac{1}{2}(N^2 + 3N + 2) \quad (2)$$

local settings. It is not possible to perform such a tomography with fewer settings.

*Proof.*—First, we need to understand the information obtainable from a single measurement setting. We assume that for every given setting, the same basis is measured at every site [14]. Measuring a local basis  $\{|\phi_1\rangle, |\phi_2\rangle\}$  is equivalent to estimating the expectation value of the traceless operator  $A = |\phi_1\rangle\langle\phi_1| - |\phi_2\rangle\langle\phi_2|$ . Merely by measuring  $A^{\otimes N}$ , it is possible to obtain all the  $N$  expectation values

$$\langle\langle A^{\otimes(N-n)} \otimes \mathbb{1}^{\otimes n} \rangle\rangle_{\text{PI}}, \quad (n = 0, \dots, N-1), \quad (3)$$

and, conversely, that is all the information obtainable about  $\varrho_{\text{PI}}$  from a single setting.

Next, we will use the fact that any PI density operator can be written as a linear combination of the pairwise orthogonal operators  $(X^{\otimes k} \otimes Y^{\otimes l} \otimes Z^{\otimes m} \otimes \mathbb{1}^{\otimes n})_{\text{PI}}$ , where  $X$ ,  $Y$ , and  $Z$  are the Pauli matrices. We consider the space spanned by these operators for one specific value of  $n$ . Simple counting shows that its dimension is  $\mathcal{D}_{(N-n)}$ . The same space is spanned by  $\mathcal{D}_{(N-n)}$  generic operators of the type  $(A_j^{\otimes(N-n)} \otimes \mathbb{1}^{\otimes n})_{\text{PI}}$ . We draw two conclusions: First, any setting gives at most one expectation value for every such space. Hence the number of settings cannot be smaller than the largest dimension, which is  $\mathcal{D}_N$ . Second, a generic choice of  $\mathcal{D}_N$  settings is sufficient to recover the correlations in each of these spaces, and hence completely characterizes  $\varrho_{\text{PI}}$ . This concludes the proof [15].

The proof implies that there are real coefficients  $c_j^{(k,l,m)}$  such that

$$\begin{aligned} &\langle\langle X^{\otimes k} \otimes Y^{\otimes l} \otimes Z^{\otimes m} \otimes \mathbb{1}^{\otimes n} \rangle\rangle_{\text{PI}} \\ &= \sum_{j=1}^{\mathcal{D}_N} c_j^{(k,l,m)} \langle\langle A_j^{\otimes(N-n)} \otimes \mathbb{1}^{\otimes n} \rangle\rangle_{\text{PI}}. \end{aligned} \quad (4)$$

We will refer to the numbers on the left-hand side of Eq. (4) as the elements of the generalized Bloch vector. The expectation values on the right-hand side can be obtained by measuring the settings with  $A_j$  for  $j = 1, 2, \dots, \mathcal{D}_N$ .

*Minimizing uncertainties.*—We now have to determine the optimal scheme for PI tomography. To this end, we define our measure of statistical uncertainty as the sum of the variances of all the Bloch vector elements

$$\begin{aligned} (\mathcal{E}_{\text{total}})^2 &= \sum_{k+l+m+n=N} \mathcal{E}^2[(X^{\otimes k} \otimes Y^{\otimes l} \otimes Z^{\otimes m} \otimes \mathbb{1}^{\otimes n})_{\text{PI}}] \\ &\times \left( \frac{N!}{k!l!m!n!} \right), \end{aligned} \quad (5)$$

where the term with the factorials is the number of different permutations of  $X^{\otimes k} \otimes Y^{\otimes l} \otimes Z^{\otimes m} \otimes \mathbb{1}^{\otimes n}$ . Based on Eq. (4), the variance of a single Bloch vector element is

$$\begin{aligned} &\mathcal{E}^2[(X^{\otimes k} \otimes Y^{\otimes l} \otimes Z^{\otimes m} \otimes \mathbb{1}^{\otimes n})_{\text{PI}}] \\ &= \sum_{j=1}^{\mathcal{D}_N} |c_j^{(k,l,m)}|^2 \mathcal{E}^2[(A_j^{\otimes(N-n)} \otimes \mathbb{1}^{\otimes n})_{\text{PI}}]. \end{aligned} \quad (6)$$

Equation (5) can be minimized by changing the  $A_j$  matrices and the  $c_j^{(k,l,m)}$  coefficients. We consider the coefficients first.

For any Bloch vector element, finding  $c_j^{(k,l,m)}$ 's that minimize the variance Eq. (6) subject to the constraint that equality holds in Eq. (4) is a least squares problem. It has an analytic solution obtained as follows: Write the operator on the left-hand side of Eq. (6) as a vector  $\vec{v}$  (with respect to some basis). Likewise, write the operators on the right-hand side as  $\vec{v}_j$  and define a matrix  $V = [\vec{v}_1, \vec{v}_2, \dots, \vec{v}_{\mathcal{D}_N}]$ . Then Eq. (4) can be cast into the form  $\vec{v} = V\vec{c}$ , where  $\vec{c}$  is a vector of the  $c_j^{(k,l,m)}$  values for given  $(k, l, m)$ . If  $E$  is the diagonal matrix with entries  $E_{j,j}^2 = \mathcal{E}^2[(A_j^{\otimes(N-n)} \otimes \mathbb{1}^{\otimes n})_{\text{PI}}]$ , then the optimal solution is  $\vec{c} = E^{-2}V^T(VE^{-2}V^T)^{-1}\vec{v}$ , where the inverse is taken over the range [16].

Equipped with a method for obtaining the optimal  $c_j^{(k,l,m)}$ 's for every fixed set of observables  $A_j$ , it remains to find the best settings to measure. Every qubit observable can be defined by the measurement directions  $\vec{a}_j$  using  $A_j = a_{j,x}X + a_{j,y}Y + a_{j,z}Z$ . Thus, the task is to identify  $\mathcal{D}_N$  measurement directions on the Bloch sphere minimizing the variance. In general, finding the globally optimal solution of high-dimensional problems is difficult. In our case, however,  $\mathcal{E}_{\text{total}}$  seems to penalize an inhomogeneous distribution of the  $\vec{a}_j$  vectors; thus, using evenly distributed vectors as an initial guess, usual minimization procedures can be used to decrease  $\mathcal{E}_{\text{total}}$  and obtain satisfactory results [16].

The variance  $\mathcal{E}^2[(A_j^{\otimes(N-n)} \otimes \mathbb{1}^{\otimes n})_{\text{PI}}]$  of the observed quantities depends on the physical implementation. In the photonic setup below, we assume Poissonian distributed counts. It follows that (see also Refs. [17,18])

$$\mathcal{E}^2[(A_j^{\otimes(N-n)} \otimes \mathbb{1}^{\otimes n})_{\text{PI}}] = \frac{[\Delta(A_j^{\otimes(N-n)} \otimes \mathbb{1}^{\otimes n})_{\text{PI}}]_{\varrho_0}^2}{\lambda_j - 1}, \quad (7)$$

where  $(\Delta A)_{\varrho}^2 = \langle A^2 \rangle_{\varrho} - \langle A \rangle_{\varrho}^2$ ,  $\varrho_0$  is the state of the system, and  $\lambda_j$  is the parameter of the Poissonian distribution, which equals the expected value of the total number of counts for the setting  $j$ . The variance depends on the unknown state. If we have preliminary knowledge of the likely form of  $\varrho_0$ , we should use that information in the optimization. Otherwise,  $\varrho_0$  can be set to the completely mixed state. For the latter, straightforward calculation shows that  $\mathcal{E}^2[(A_j^{\otimes(N-n)} \otimes \mathbb{1}^{\otimes n})_{\text{PI}}] = \binom{N}{n}^{-1}/(\lambda_j - 1)$ . For another implementation, such as trapped ions, our scheme for PI tomography can be used after replacing Eq. (7) by a formula giving the variance for that implementation.

*Estimating the information loss due to symmetrization.*—It is important to know how close the PI quantum state is to the state of the system as PI tomography should

serve as an alternative of full state tomography for experiments aiming at the preparation of PI states.

**Observation 2.** The fidelity between the original state and the permutationally invariant state,  $F(\varrho, \varrho_{PI})$ , can be estimated from below as  $F(\varrho, \varrho_{PI}) \geq \langle P_s \rangle_{\varrho}^2$ , where  $P_s = \sum_{n=0}^N |D_N^{(n)}\rangle\langle D_N^{(n)}|$  is the projector to the  $N$ -qubit symmetric subspace, and the symmetric Dicke state is defined as  $|D_N^{(n)}\rangle = \binom{N}{n}^{-1/2} \sum_k \mathcal{P}_k(|0\rangle^{\otimes(N-n)} \otimes |1\rangle^{\otimes n})$ , where the summation is over all the different permutations of the qubits. Observation 2 can be proved based on Ref. [19] and elementary matrix manipulations. Note that Observation 2 makes it possible to estimate  $F(\varrho, \varrho_{PI})$  based on knowing only  $\varrho_{PI}$ .

Lower bounds on the fidelity to symmetric Dicke states, i.e.,  $\text{Tr}(|D_N^{(n)}\rangle\langle D_N^{(n)}| \varrho)$  can efficiently be obtained by measuring  $X$ ,  $Y$ , and  $Z$  on all qubits, i.e., measuring only three local settings independent of  $N$  [20]. With the same measurements, one can also obtain a lower bound on the overlap between the state and the symmetric subspace. For four qubits, this can be done based on  $P_s \geq [(J_x^4 + J_y^4 + J_z^4) - (J_x^2 + J_y^2 + J_z^2)]/18$ , where  $J_x = (1/2)\sum_k X_k$ ,  $J_y = (1/2)\sum_k Y_k$ , etc. Operators for estimating  $\langle P_s \rangle$  for  $N = 6, 8$  are given in Ref. [16]. This allows one to judge how suitable the quantum state is for PI tomography before such a tomography is carried out.

*Experimental results.*—We demonstrate the method and the benefits of our algorithm for PI tomography for a four-qubit symmetric Dicke state with two excitations  $|D_4^{(2)}\rangle$ . First, we optimize the  $\vec{a}_j$ 's and the  $c_j^{(k,l,m)}$ 's for  $\varrho_0 = \mathbb{1}/16$  and only for the uncertainty of full four-qubit correlation terms, which means that when computing  $\mathcal{E}_{\text{total}}$ , we carry out the summation in Eq. (5) only for the terms with  $n = 0$ . With simple numerical optimization, we were looking for the set of  $A_j$  basis matrices that minimize the uncertainty of the full correlation terms. Then, we also looked for the basis matrices that minimize the sum of the squared error of all the Bloch vector elements and considered also density matrices different from white noise, such as a pure Dicke state mixed with noise. We find that the gain in terms of decreasing the uncertainties is negligible in our case and that it is sufficient to optimize for  $\varrho_0 = \mathbb{1}/16$  and for the full correlation terms. To demonstrate the benefits of the optimization of the measurement directions, we also compare the results with those obtained with randomly distributed basis matrices.

The Dicke state was observed in a photonic system. Essentially, four photons emitted by the second-order collinear type-II spontaneous parametric down-conversion process were symmetrically distributed into four spatial modes. Upon detection of one photon from each of the outputs, the state  $|D_4^{(2)}\rangle$  is observed. Polarization analysis in each mode is used to characterize the experimentally observed state. We collected data for each setting for 5 min, with an average count rate of 410 per minute. The experimental setup has been described in detail in Refs. [2,3].

First, to check the applicability of the PI tomography, we apply our tools described above requiring only the

measurement of the three settings,  $X^{\otimes 4}$ ,  $Y^{\otimes 4}$ , and  $Z^{\otimes 4}$ . We determine the expectation value of the projector to the symmetric subspace, yielding  $\langle P_s \rangle \geq 0.905 \pm 0.015$ . Based on Observation 2, we obtain  $F(\varrho, \varrho_{PI}) \geq 0.819 \pm 0.028$ . These results show that the state is close to be PI and has a large overlap with the symmetric subspace. Thus, it makes sense to apply PI tomography.

For PI tomography of a four-qubit system, the measurement of 15 settings is needed. We used Eq. (4) to obtain the Bloch vector elements from the experimentally measured quantities. This way, we could obtain all the 34 symmetric correlations of the form  $(X^{\otimes k} \otimes Y^{\otimes l} \otimes Z^{\otimes m} \otimes \mathbb{1}^{\otimes n})_{PI}$ . In Fig. 1, we give the values of the correlations for optimized and for randomly chosen measurement directions, compared to the results obtained from full tomography, which needed 81 measurement settings. As can be seen in Fig. 1, the uncertainty for the optimized settings is considerably smaller than the one for the randomly chosen settings. Moreover, the results from the optimized settings fit very well the results of the full tomography. In Fig. 2, we compare the density matrices obtained from full tomography [Fig. 2(a)], from PI tomography for optimized [Fig. 2(b)], and for random measurement directions [Fig. 2(c)]. Because of noise, the fidelity of the result of the full tomography with respect to  $|D_4^{(2)}\rangle$  is  $0.873 \pm 0.005$ , which is similar to the fidelity of the results of the PI tomography with optimized settings,  $0.852 \pm 0.009$  [21]. In contrast, for the method using random measurement directions, the fidelity is  $0.814 \pm 0.059$ , for which the

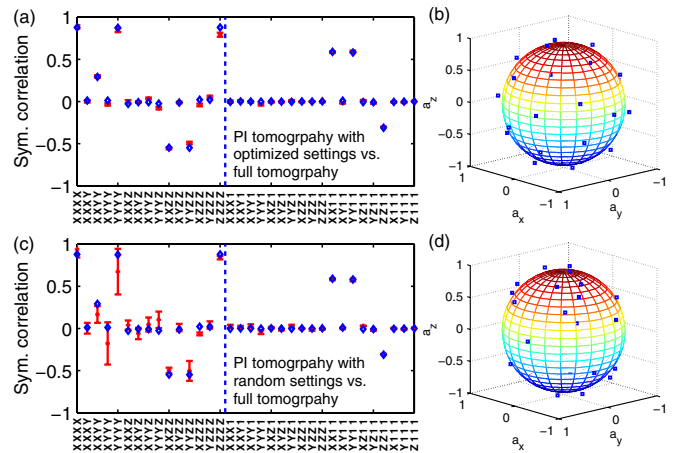


FIG. 1 (color online). (a) Comparison of the 34 symmetrized correlations coming from (crosses with error bars) 15 permutationally invariant measurement settings with optimized  $A_j$  matrices for  $N = 4$  qubits and (diamonds) from full tomography requiring 81 local settings. The average uncertainty of all symmetrized correlations obtained from full tomography is  $\pm 0.022$ , and is not shown in the figure. The labels refer to symmetrized correlations of the form given in the left-hand side of Eq. (4). The results corresponding to the 15 full four-qubit correlations are left from the vertical dashed line. (b) Measurement directions. A point at  $(a_x, a_y, a_z)$  corresponds to measuring operator  $a_x X + a_y Y + a_z Z$ . (c) Results for randomly chosen  $A_j$  matrices and (d) corresponding measurement directions.

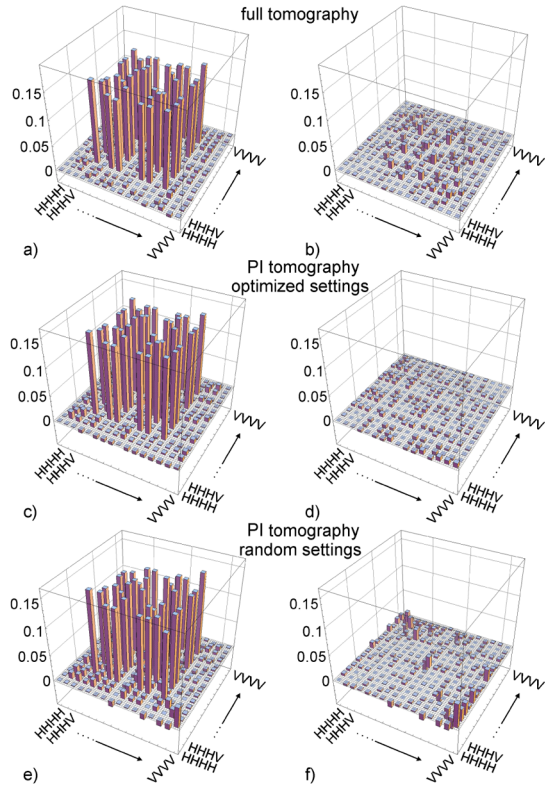


FIG. 2 (color online). (a) The real and (b) imaginary parts of the density matrix coming from full tomography. (c),(d) The same for permutationally invariant tomography with optimized and (e),(f) random measurement directions, respectively.

uncertainty is the largest compared to all previous fidelity values. Finally, we also computed the fidelity of the results with respect to the PI density matrix obtained from full tomography [22]. The results of the PI tomography with optimized settings show a good agreement with full tomography: the fidelity is 0.947, which is quite close to the fidelity between the results of full tomography and its PI part, 0.964. On the other hand, for the PI tomography with random settings the corresponding fidelity is much lower, 0.880. Overall, the PI tomography shows a good agreement with the full tomography for this particular experiment. However, a reasonable choice of measurement directions is needed to obtain uncertainties in the reconstructed Bloch vector elements similar to the ones from full tomography.

Finally, let us comment on how our method can be extended to larger systems. Permutationally invariant operators can be represented efficiently on a digital computer in the basis of  $(X^{\otimes k} \otimes Y^{\otimes l} \otimes Z^{\otimes m} \otimes \mathbb{1}^{\otimes n})_{\text{PI}}$  operators. We determined the optimal  $A_j$  operators for PI tomography for systems with  $N = 6, 8, \dots, 14$  qubits. To have the same maximum uncertainty of the Bloch vector elements as for the  $N = 4$  case, one has to increase the counts per setting by less than 50% [16].

In summary, we presented a scalable method for permutationally invariant tomography, which can be used in place of full state tomography in experiments that aim at preparing permutationally invariant many-qubit states. For our approach, the same operator has to be measured on all qubits,

which is a clear advantage in some experiments. We showed how to choose the measurements such that the uncertainty in the reconstructed density matrix is the smallest possible. This paves the way of characterizing permutationally invariant states of many qubits in various physical systems. Moreover, this work also shows that, given some knowledge or justifiable assumptions, there is a way to obtain scalable state tomography for multiqubit entangled states.

We thank D. Hayes and N. Kiesel for discussions. We thank the Spanish MEC (Consolider-Ingenio 2010 project "QOIT," Project No. FIS2009-12773-C02-02), the Basque Government (Project No. IT4720-10), the ERC StG GEDENTQOPT, the DFG-Cluster of Excellence MAP, the EU projects QAP, Q-Essence, and CORNER, and the DAAD/MNISW for support. W.W. and C.S. thank the QCCC of the Elite Network of Bavaria for support.

\*Present address: Faculty of Physics, University of Vienna, Boltzmanngasse 5, A-1090 Wien, Austria.

- [1] J.-W. Pan *et al.*, *Nature (London)* **403**, 515 (2000); M. Bourennane *et al.*, *Phys. Rev. Lett.* **92**, 087902 (2004); N. Kiesel *et al.*, *ibid.* **95**, 210502 (2005).
- [2] N. Kiesel *et al.*, *Phys. Rev. Lett.* **98**, 063604 (2007).
- [3] W. Wieczorek *et al.*, *Phys. Rev. Lett.* **103**, 020504 (2009); R. Krischek *et al.*, *Nat. Photon.* **4**, 170 (2010).
- [4] R. Prevedel *et al.*, *Phys. Rev. Lett.* **103**, 020503 (2009).
- [5] W. Wieczorek *et al.*, *Phys. Rev. Lett.* **101**, 010503 (2008).
- [6] C. A. Sackett *et al.*, *Nature (London)* **404**, 256 (2000); H. Häffner *et al.*, *Nature (London)* **438**, 643 (2005).
- [7] O. Mandel *et al.*, *Nature (London)* **425**, 937 (2003).
- [8] C. Cinelli *et al.*, *Phys. Rev. Lett.* **95**, 240405 (2005); G. Vallone *et al.*, *ibid.* **98**, 180502 (2007); W.-B. Gao *et al.*, *Nature Phys.* **6**, 331 (2010).
- [9] For other approaches see D. Gross *et al.*, *Phys. Rev. Lett.* **105**, 150401 (2010); M. Cramer and M. B. Plenio, *arXiv:1002.3780*; S. T. Flammia *et al.*, *arXiv:1002.3839*; O. Landon-Cardinal *et al.*, *arXiv:1002.4632*.
- [10] G. M. D'Ariano *et al.*, *J. Opt. B* **5**, 77 (2003).
- [11] R. B. A. Adamson *et al.*, *Phys. Rev. Lett.* **98**, 043601 (2007).
- [12] L. K. Shalm *et al.*, *Nature (London)* **457**, 67 (2009).
- [13] O. Gühne and G. Tóth, *Phys. Rep.* **474**, 1 (2009).
- [14] Otherwise more than  $\mathcal{D}_N$  settings are necessary [16].
- [15] This is connected to a general idea: It is expected that the determination of an operator within a subspace whose dimension depends polynomially on  $N$  needs a number of settings increasing also polynomially with  $N$ .
- [16] See supplementary material at <http://link.aps.org/supplemental/10.1103/PhysRevLett.105.250403> for additional derivations and experimental results.
- [17] C. Schmid, Ph.D. thesis, Ludwig-Maximilian-Universität, 2008; D. F. V. James *et al.*, *Phys. Rev. A* **64**, 052312 (2001).
- [18] B. Jungnitsch *et al.*, *Phys. Rev. Lett.* **104**, 210401 (2010).
- [19] J. A. Miszczak *et al.*, *Quantum Inf. Comput.* **9**, 0103 (2009).
- [20] G. Tóth *et al.*, *New J. Phys.* **11**, 083002 (2009).
- [21] Expectation values are obtained directly from the measured data, rather than from  $\rho_{\text{PI}}$ .
- [22] Values without error are deduced from fitted matrices obtained via maximum likelihood estimation [17].